Spectrum Journal of Innovation, Reforms and Development
Volume 42, August 2025 | ISSN (E): 2751-1731
WEBSITE: WWW.SJIRD.JOURNALSPARK.ORG

PERFORMANCE ANALYSIS OF HELICAL COIL AND INNOVATIVE TUBES HEAT EXCHANGER WITH PHASE CHANGE MATERIALS: NUMERICAL AND EXPERIMENTAL STUDY

Atheer S. Hassoon 1*
1 Power Mechanics Techniques Engineering Department, Al-Musaib Technical College, Al-Furat Al-Awsat Technical University (ATU), Kufa 54001, Iraq
* Corresponding author: atheer.hassoon@atu.edu.iq

Abstract
This study presents a numerical and experimental analysis of two models of latent heat storage systems using heat exchangers with phase change material (PCM). The models utilized were helically coiled tube heat exchangers (HCT-HX) and innovative tube heat exchangers (IT-HX). The models were analyzed for two distinct injections of Heat Transfer Fluid (HTF) from the upper section of the models. The comparison of both scenarios showed that varying the Heat Transfer Fluid inlet while maintaining a constant mass flow rate significantly influences the duration of the melting process. In comparison, the melting time for (HCT-HX) decreases by 11.2%, whereas (IT-HX) results in a 24% delay in melting. The model in (HCT-HX) has the best thermal performance and the quickest melting time because of the geometry of it. A high degree of concordance was seen when the numerical and experimental outcomes were compared.

Keywords: IT-HX, HCT-HX, PCM, melting time, latent heat storage.

Introduction

Solar energy is one tool in the fight against the energy problem, but its unreliability makes it less respectable and dependable than more conventional options. Consequently, it would appear that the requirement for thermal energy storages is driving up solar energy's acceptability; these storages capture thermal energy when it's abundant and put it to use when it's scarce. It is preferable to convert thermal energy into latent heat rather than sensible heat for some materials since the latent heat is substantially larger [1]. Phase Change Materials (PCM) are the building blocks of latent heat storage systems. Their moniker comes from the fact that, when they undergo a melting and solidification cycle during charging and discharging, their phase changes. PCM undergoes a phase transition from solid to liquid and back again throughout the melting and solidification processes; during the former, it absorbs heat from its perimeter, and during the latter, it releases heat, transforming back into a solid. The thermal energy that is either emitted or absorbed during the PCM's phase shift is known as latent heat [2-4].

One major issue with employing PCM for storing heat was their low thermal conductivity, which slows down the charging and discharging rates and impacts the phase transition. Because of this, the prospect of storing and recovering thermal energy is severely diminished. As a result,

enhancing heat transmission is one of the necessary and vital steps. This issue can only be resolved by utilizing materials that enhance PCM heat transmission, such as stable solid inserts made of graphene or metallic arrays [5,6].

Numerous previous studies aimed to discover the optimal method for transferring the most quantity of heat generated by the heat-storage medium to the heat transfer medium. Finding the most suitable PCM- for example, paraffin wax- has been the subject of several studies, while others have suggested optimized heat exchanger designs [7].

An experimental assessment of the thermal performance was conducted on two distinct finned Systems for latent heat storage, one with circular fins and the other with longitudinal fins [8]. Results shown that overall charging time may be reduced by 69% with circular fins and by 55% with longitudinal fins. Additionally, they found that circular fins improved cumulative energy storage by about 52% when compared to longitudinal fins.

For the purpose of melt paraffin in thermal containers, a three-dimensional computational and experimental investigation was carried out [9]. The vertically oriented modified test module features a 3 mm PVC casing and a 0.5 mm thick copper nozzle. A ten-millimeter-thick covering of Styrofoam shields the models from dampness. When comparing both the experimental and numerical findings of the temperature (Temp) distribution, there was a good agreement. Additionally, it has been proven that the nozzle-and-shell model had the best melting process when compared to other models. Although reducer-and-shell was the most inefficient. Analyze and compare the phases of latent heat thermal storage's melting and solidification in a solar water heating system. Using an evacuated heat pipe and latent heat storage, they propose a novel design for a solar water heater that saves space. Compared to the baseline, the proposed system was around 10%-58% more efficient across all three PCMs [10].

Employing fins and nanoparticles. [11] expedited the phase change material discharge of a heat exchanger in thermal power storage with a triple-pipe. PCM was analyzed numerically as a medium for thermal storage in a solar water collector [12]. The CFD predictions align well with the previously evaluated and publicized experimental data referenced in [13]. A theoretical and experimental study was conducted by [14] to investigate the melting of a phase-change material in a heat exchanger using a triplex tube with longitudinal and triangle fins. External triangle fins improved performance by 15%, external-internal fins by 12%, and internal triangle fins by 11%. The phase-change materials (PCM) with longitudinal fins and triangle fins were tested for energy storage capacities; the results showed that the triangle tube with external fins was the most effective for rapid PCM melting.

A numerical study is performed on both models: a cylindrical form and a tube with comparable heat transfer regions inside a tube and shell heat exchanger [15]. The results were evaluated for vertical and horizontal types with varying fluid intake. When the model was placed vertically with the heat transfer fluid input at the base, the thermal storage and melting rate were optimized. The results showed that the horizontal cylinder outperformed the horizontal tube. [16] performed theoretical and experimental research on a vertical thermal storage model, comparing the conical and cylindrical geometries of tube and shell heat exchangers during both charging and discharging. The findings showed that the conical geometry charged faster than the cylindrical geometry, although there was little difference between the two models when discharging.

According to the abovementioned research, heat exchangers are crucial for thermal energy storages, and PCMs play a key role in improving the thermal performance of these spaces. Consequently, this study aims to use two models HCT-HX and IT-HX to conduct an experimental and numerical examination of thermal energy storage.

2. Physical Models and Numerical Work

The helical coil and innovative pipe arrangement, covered in an insulated shell as seen in Figure 1, are designed by SOLIDWORKS software to examine the transient heat transfer processes associated with the melting and solidification of paraffin, as well as to compare the models regarding their thermal performance. The hot water circulates through the inner molds, with the paraffin wax (PCM amount is equal in the two models) in direct contact with these molds within the shell.

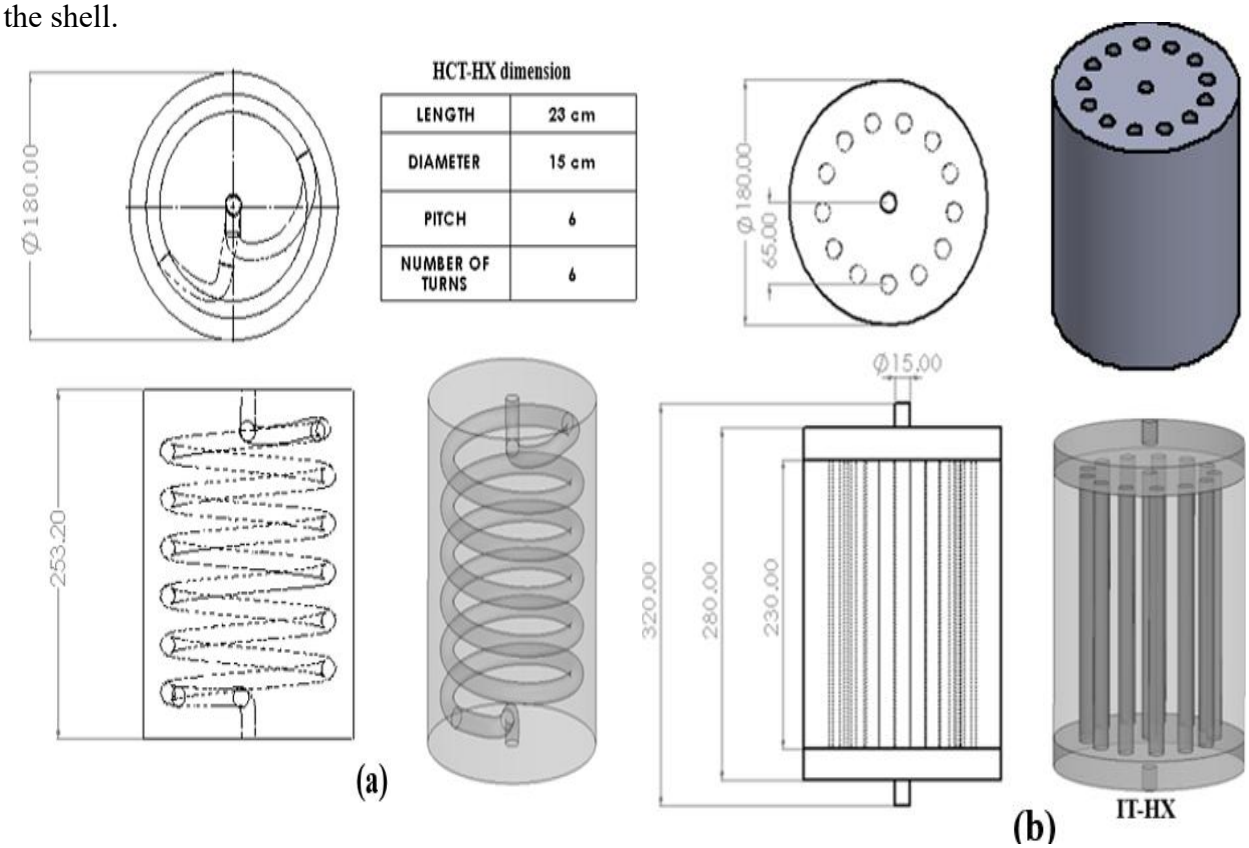

Fig. 1. Physical layouts of the (a) HCT-HX, (b) IT-HX (all dimensions are in cm).

The utilized (PCM) is paraffin, characterized by the parameters shown in Table I. The (HTF) is water introduced from the upper section of the models to the lower section.

Table 1. Thermal Characteristics of utilized paraffin wax.

Fig. 1. Melting Temp Range (K)	Fig. 2. 321-335
Fig. 3. Specific heat (J/kg·K)	Fig. 4. 2000
Fig. 5. Heat of fusion (J/kg)	Fig. 6. 114540
Fig. 7. Viscosity coefficient (kg/(m·s))	Fig. 8. 0.033
Fig. 9. Conductivity (W/m·K)	Fig. 10. 0.14
Fig. 11. Thermal expansion coefficient (1/K)	Fig. 12. $6*10^{-4}$
Fig. 13. Density (kg/m^3)	Fig. 14. 820

In this study, the enthalpy method is employed for numerical simulation to predict the phase transition behavior of phase change materials (PCM) without the need for explicit tracking of the solid–liquid interface. The approach inherently accounts for the intermediate region between the two phases, known as the mushy zone, enabling a more direct treatment of the phase transition process by utilizing governing equations analogous to those of single-phase flow and heat transfer (Hosseini et al., 2014). The numerical model is formulated dependent on the transient Navier–Stokes equations, incorporating the energy, momentum, and continuity equations, and is developed under the following assumptions: (i) the PCM is homogeneous and isotropic; (ii) the heat transfer fluid (HTF) exhibits Newtonian and incompressible flow characteristics; (iii) the thermal resistance of the tube wall is negligible due to the high thermal conductivity of the metallic material; (iv) the thermophysical properties of both PCM and HTF are temperature-independent, although distinct for the solid and liquid phases of the PCM; (v) heat loss from the system is negligible, implying that the outer surface of the shell is perfectly thermally insulated; and (vi) axial conduction in both the HTF and PCM is negligible. This modeling framework enables accurate and computationally efficient analysis of coupled heat transfer and phase change phenomena in latent heat thermal energy storage systems.

According to [18,19], the continuity equation used in this study takes the following form:

$$\frac{\partial \rho}{\partial t} + \nabla.\left(\rho \vec{V}\right) = 0 \qquad (1)$$

Whereas (V, ρ, and t) denote the velocity, density, and time of PCM, respectively.

According to [20], the momentum equations are as follows:

$$\rho\left(\frac{\partial \vec{V}}{\partial t} + \left(\nabla.\vec{V}\right)\vec{V}\right) = \mu\left(\nabla^2\vec{V}\right) - \nabla P + \frac{(1-\beta)^2}{(\beta^3+€)^3} A_{mush}\vec{V} + \rho\vec{g}\gamma(T - T_0) \qquad (2)$$

Where μ is the viscosity of the PCM and P is the pressure. The solid PCM in the mushy zone is represented by the third term in the right-hand side, since (€) is a small number used to obviate division by zero [21]. The constant of a mushy zone; A_{mush} is set at the magnitude that gives the best simulation results, which is 105 kg/m3s [22]. $\vec{g}$ and T_0 are the gravitational acceleration and the operating Temp.

The energy equation is defined by [23]:

$$\frac{\partial}{\partial t}(\rho h) + \nabla.\left(\rho \vec{V} h\right) = \nabla.(K \nabla T) + \frac{\partial(\rho \nabla h)}{\partial t} + \nabla.\left(\rho \vec{V} h\right) \qquad (3)$$

Where t, T, ρ, V, and K are time, the local Temp, local density, velocity, and thermal conductivity of PCM, h is a sensible enthalpy [24];

$$h = h_{ref} + \int_{T_{ref}}^{T} C\, dT + \beta L \qquad (4)$$

Where T_{ref} refers to the reference Temp, h_{ref} refers to the enthalpy at the reference Temp, L and C refer to the liquid PCM heat (specific and latent). β refers to the liquid fraction of the mushy zone whereas its magnitude in this zone ranges from 0 to 1 [25];

$$\beta = 0 \qquad \text{for} \quad T < T_{solidus}$$

$$\beta = \frac{T - T_{solidus}}{T_{liquidus} - T_{solidus}} \qquad \text{for} \quad T_{solidus} < T < T_{liquidus}$$

$$\beta = 1 \qquad \text{for} \quad T > T_{liquidus} \qquad (5)$$

The models were meshed using ANSYS FLUENT 2021 R1 as shown in Figure 2, evaluating three distinct cell sizes (0.5, 0.8, and 1). The cell size of 0.8 was selected to optimize result accuracy and computational efficiency. A time step of 1 was chosen from the available options (0.5, 1, and 2) for the current simulations.

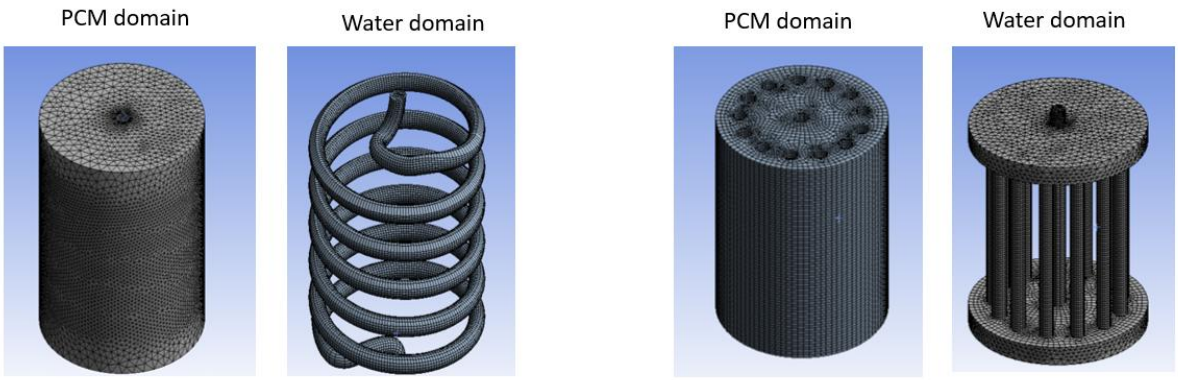

Fig. 2. Mashing domain for HCT-HX and IT-HX.

3. Experimental Work

3.1 Experimental Setup

Figure 3 illustrates the schematic design of the experimental setup. The system predominantly comprises a tube and shell heat exchanger, a thermal bath containing a 70 L water tank fitted with a 500 W electric heater, an 8 mm diameter copper pipe, thermocouples of the K type with a precision of ± 0.15℃ and a Temp range of 0-200℃, a turbine flow meter with an accuracy of 0.25%, and an 8-channel multi-channel data logger. The experimental configuration included a 0.37 KW Melto Power circulation pump, accompanied by the necessary pipework and valves for water flow management. The experimental PCM storage test section has two heat exchanger designs housed inside a transparent cylindrical Perspex shell: the helical coil tube and the novel tube system.

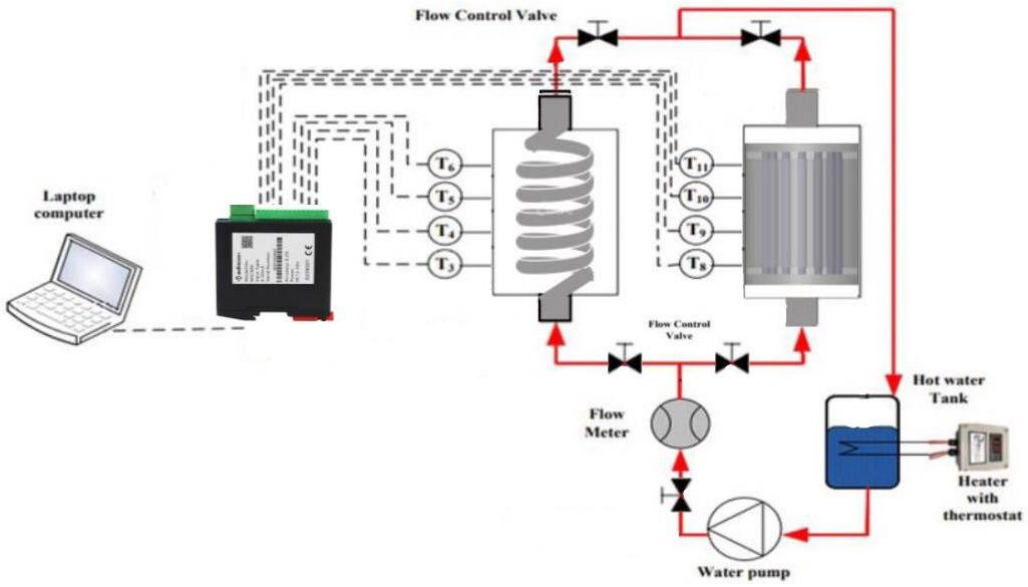

Fig. 3. Schematic diagram and the apparatus of the experimental work.

3.2 Test Procedure

The following steps describe the strategy for this task:

1. Fill the test portions with paraffin wax to a height of 20 cm.
2. Fill the tank with water up to three-quarters full.
3. Activate the heater and adjust the thermostat to 60℃.
4. Activate the circulating pump when the water attains a Temp of 60℃.
5. Regulate the flow rate using the valves, first setting it to 3 liters per minute and adjusting the flow rate to remaining at 3 liters per minute.
6. Measure the Temp using a Temp measurement device linked to the computer every 5 minutes to preserve the readings immediately.

3.3 Uncertainty Analysis

In error analysis, a number of independent and dependent factors are used to quantify the measurement errors in the experimental data. These variables include Temp, flowmeter, enthalpy, and liquid fraction. One way to assess the mistakes made by these variables (W_{R^+}) is as follows [26]:

$$W_{R^+} = \sqrt[2]{(\frac{\delta R^+}{\delta X_1} w_1)^2 + (\frac{\delta R^+}{\delta X_2} w_2)^2 + \cdots + (\frac{\delta R^+}{\delta X_n} w_n)^2} \qquad (6)$$

If the independent error variable is w1, w2 …wn, and the independent variables X1, X2 …Xn determine R+. A thorough summary of the study's main results is given in Table 1.

Table 2. Absolute Accuracy

Fig. 15.	Independent variables	Fig. 16.	Variable errors
Fig. 17.	Inlet water Temp (℃)	Fig. 18.	∓0.03
Fig. 19.	Outlet water Temp (℃)	Fig. 20.	∓0.03
Fig. 21.	Temp of PCM (℃)	Fig. 22.	∓0.036
Fig. 23.	Dependent variables	Fig. 24.	Variable errors
Fig. 25.	Liquid friction (-)	Fig. 26.	∓0.05

4. Results and Discussions

Figure 4 depicts the anticipated outcomes from the numerical simulation of the Temp distribution over time for HCT-HX. The paraffin Temp begins at 300 K, while the water flow is at 340 K with a mass flow rate of 3 L/min. Subsequently, the paraffin Temp rose with the passage of time. The Temp near the nozzle surface increased more rapidly as heat transfer occurred, imparting sensible heat to the paraffin in its solid state. The Temp stabilizes, signifying that the paraffin absorbs heat and raises its original Temp to the melting point, facilitating the phase transition from solid to liquid. The Temp often remains constant over time, representing the presence of latent heat in the paraffin. Subsequently, the paraffin Temp was raised until it matched the Temp of the hot wall. That is, the heat absorbed (sensible heat) by the liquid phase allows water moving inside the model to charge the paraffin with stored energy over time. At 3500 seconds, the Temp was rising swiftly to the melting point in the HCT-HX model, where the heat stored in the paraffin was in the form of sensible heat. Subsequently, at 6600 seconds, the paraffin begins melting at a rate surpassing that of IT-HX.

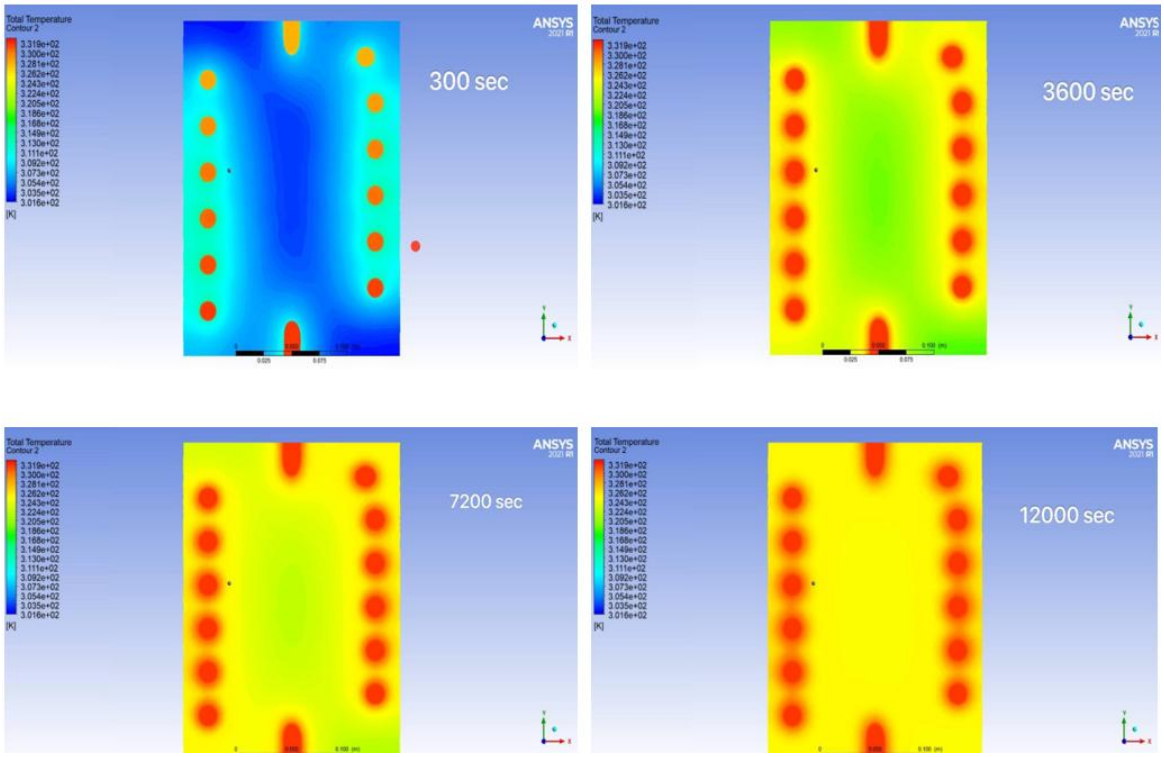

Figure 4: The paraffin CFD temp distribution contours of HCT-HX models.

Figure 5 illustrates the anticipated contours of paraffin Temp distribution during the melting process for the IT-HX models, as derived from the numerical simulation. The starting Temp of the model walls is 340 K, according to the water Temp in the flow model. Heat is conducted from the walls to the paraffin, thereby increasing with time. At 6000 seconds, the Temp was quickly ascending to the melting point in the IT-HX model, where the thermal energy contained in the paraffin was in the form of perceptible heat. Subsequently, at 8900 seconds, the paraffin exhibits a lower melting rate than both HCT and HX. The amount of paraffin sections with a nozzle exceeds that of the HCT-HX. At 8900 seconds, it is evident that the buoyancy force of liquid paraffin and the amount of paraffin exceed that of the HCT-HX.

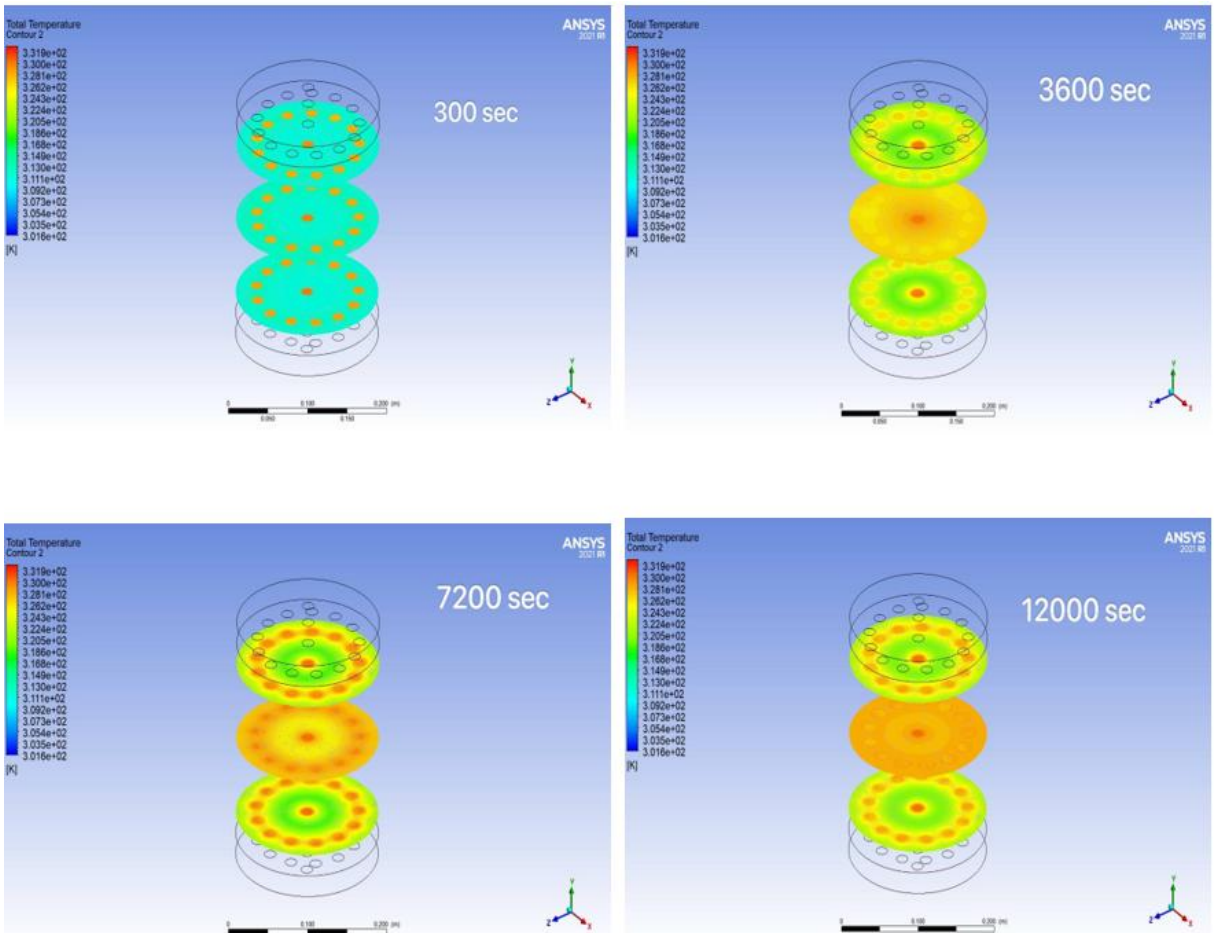

Figure 5: The paraffin CFD temp distribution contours of IT-HX models.

Figure 6 illustrates the Temp distribution for both HCT-HX and IT-HX dependent on the experimental findings. The Temp profiles for both scenarios exhibits similarities. During the initial phase of the melting process, the Temps of HCT-HX at 6000 seconds are comparable to those of IT-HX. However, in the latter phase at 9000 seconds, the Temp of HCT-HX surpasses that of IT-HX, attributable to a greater accumulation of paraffin at the upper section of the model, resulting in a delay in the melting process at that location. HCT-HX completes the melting process more rapidly than IT-HX, which failed to achieve melting at these water operational circumstances.

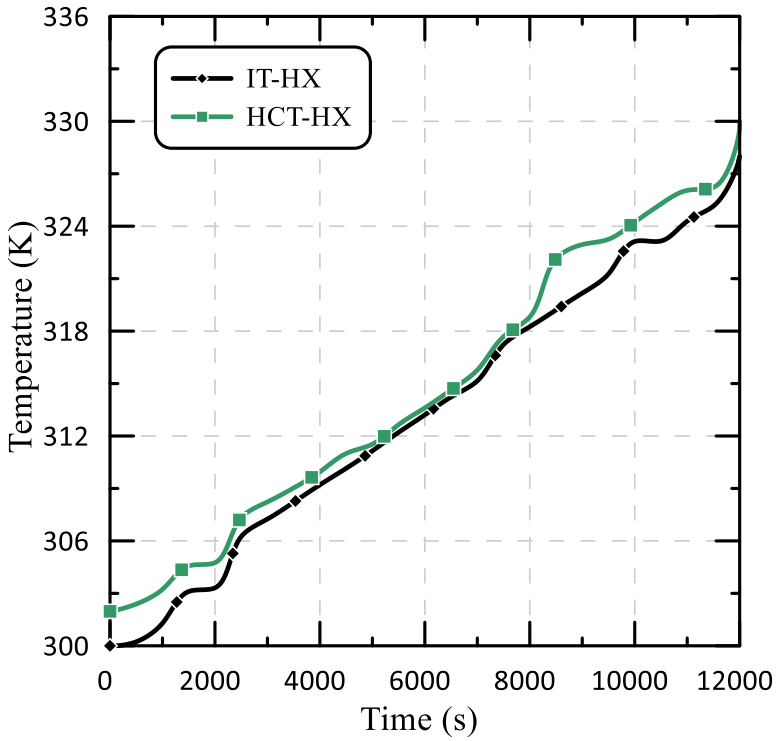

Figure 6: Temps distribution of HCT-HX and IT-HX.

Figure 7 displays the contrast between the experimental and numerical findings of paraffin temp for the HCT-HX and IT-HX models. The numerical findings closely approximate the experimental results. The temp of the paraffin with the HCT-HX is elevated compared to the IT-HX model in both computational and experimental data.

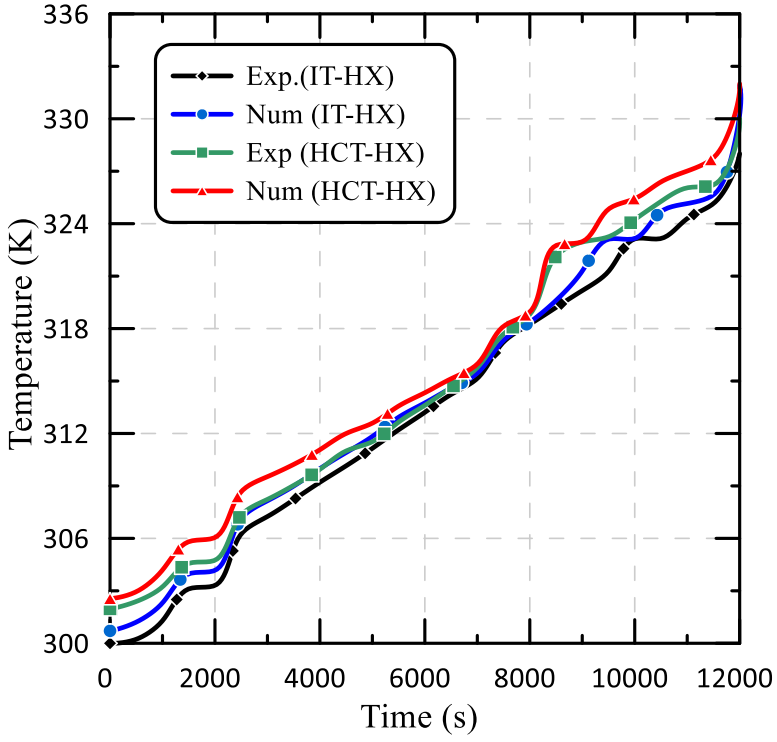

Figure 8: Numerical and Experimental temp distribution for HCT-HX and IT-HX.

Figure 8 illustrates the expected liquid fraction outcomes inside paraffin, derived from CFD simulation results and experimental data in vertical slices aligned with the water flow through the suggested models (HCT-HX) at various time intervals (300, 3600, 7200, and 12000 seconds). Initially, the melting process commenced, representing that heat was transmitted by conduction, parallel to the heated wall, mirroring the behavior described in [27].

After 300 seconds, all models exhibit paraffin in its solid form. It is shown that after 2000 and 3600 seconds, the paraffin begins melting next to the wall, with the HCT-HX model exhibiting a greater extent of melting compared to the IT-HX models.

Subsequently, when examining the numerical data at (7500 s) and (11000 s), alongside the experimental findings at (6600 s) and (8900 s) for the models, it is evident that the paraffin commenced full melting at the onset of the first half of the wall's length in the direction of flow. The HCT-HX model exhibited the fastest melting process, while the IT-HX model had the longest melting duration.

The decrease in melting time gained by the HCT-HX model is 12% and 15.7% compared to the IT-HX model, as shown by both computational and experimental findings.

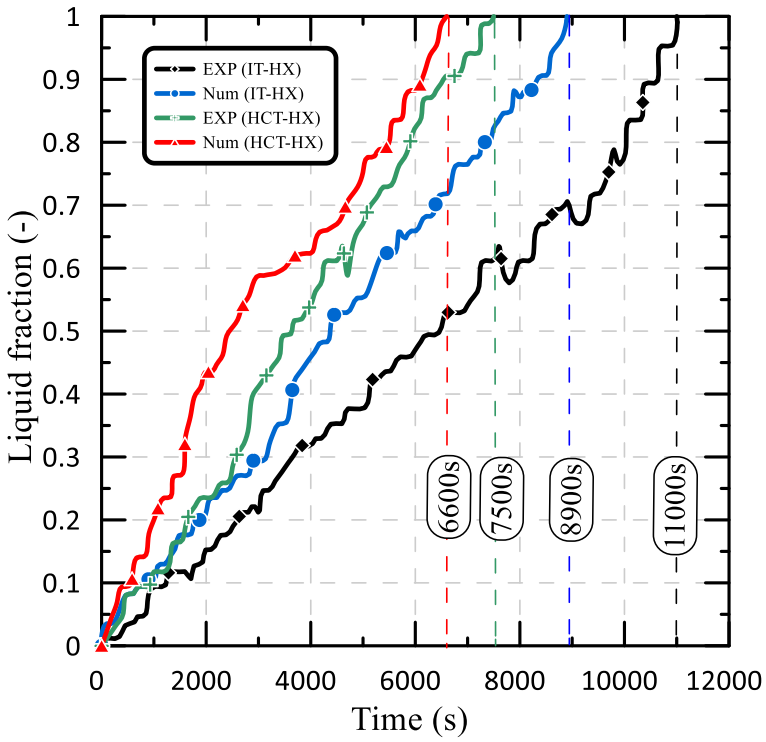

Figure 8: Numerical and Experimental Liquid Fraction for HCT-HX and IT-HX.

Generally, a reduction in the time necessary to melt the amount of paraffin, relative to the unique design of the heat exchanger, resulted in two significant advantages: The primary advantage is that time is seen as an expense; hence, its reduction signifies a decrease in the cost of the heat exchanger. The second advantage is that if the time needed for melting is used in comparison to the novel design, it suggests the feasibility of producing a smaller exchanger that delivers equivalent efficiency and performance to the unique heat exchanger. This decreases the production costs of the heat exchanger while maintaining equivalent efficiency and performance.

5. Conclusion

The study examined latent heat storage with HCT-HX and IT-HX, employing paraffin as a(PCM) and water at 340 K as the (HTF) with a mass flow rate of 3 L/min. Dependent on the quantitative and empirical findings, the following conclusions were chosen:

1. The paraffin-water system of storage has a distinct pattern compared to the paraffin-lauric acid system. The temp rose linearly, disregarding the melting point, as the solid material at 300 K transitioned immediately to the phase change material at 331.9 K within a brief duration and without resistance.
2. As temp increases, the duration of deactivation extends. As the PCM undergoes rapid melting, its melting level diminishes. The significant temp disparity between phase change materials and heat transfer fluids is primarily responsible. Enhances HTF-PCM interaction by augmenting their temp difference. Consequently, HCT-HX will exhibit a quicker melting rate than IT-HX, thus diminishing heat storage duration.
3. The overall behavior of the liquid percentage and temps for both models, in relation to the modification of the water inflow, is mostly same, with the exception of the melting completion time.
4. The HCT-HX decreases the melting time by 25%, whilst the IT-HX prolongs it by 31%.
5. In the IT-HX, 14 tubes exacerbate pressure loss while in contact with paraffin, hence impeding the melting process.

Funding: This study was not supported by any specific funding.

Data availability statement: The data that substantiate the results of this study can be obtained from the author in question on an adequate request.

Declarations

Ethical approval: It is not applicable.

Competing interests: The authors affirm that they do not have competing interests

References

1. Dzhonova-Atansova D. B., Georgiev A. G., and Popov R. K., “Numerical study of heat transfer in macro-encapsulated phase change material for thermal energy storage”, Bulgarian Chemical Communications, Vol. 48, Special Issue E, pp. 189 - 194, (2016).
2. Hiba A Hasan and Ihsan Y Hussain. Simulation and Testing of Thermal Performance Enhancement for Cascade Thermal Energy Storage System by Using Metal Foam, International Journal of Mechanical & Mechatronics Engineering IJMME-IJENS (2018) Vol:18 No:05.
3. Shivendra Singh and N. K. Sagar “A Review on Phase Change Material (PCM) Heat Exchanger with Spiral-Wired Tubes “ Journal of Advances in Science and Technology Vol. 16, Issue No. 1, March-2019, pp. (21-27).
4. Dincer and M. A. Rosen, 2002, ‘‘Thermal Energy Storage’’, Jone Wiley & Sons.
5. Mahdi JM, Nsofor EC. Melting enhancement in triplex-tube latent heat energy storage system using nanoparticles-metal foam combination. Applied Energy 2017;191:22–34.
6. Mahdi JM, Nsofor EC. Solidification enhancement in a triplex-tube latent heat energy storage system using nanoparticles-metal foam combination. Energy 2017;126:501–12.

7. Jalal M. Jalil, Hassan K. Abdullah and Kadhim H. Safar "A Numerical and Experimental Investigation into the Melting of Ice Around a Horizontal Cylinder", Dirasat, Engineering Sciences, Volume 34, No. 1, 2007, pp. (57-70).
8. Abbas Ahmed Hasan and Najim Abid Jassim. Thermal Energy Shifting Using Thermal Energy Storage with Solar Assisted System for Space Cooling Application. Al-Nahrain Journal for Engineering Sciences (NJES) Vol.23, No.3, 2020 pp.216–224: https://doi.org/10.29194/NJES.23030216.
9. Agus Dwi Korawan, Sudjito Soeparman, Widya Wijayanti, and Denny "3D Numerical and Experimental Study on Paraffin Wax Melting in Thermal Storage for the Nozzle-and-Shell, Tube-and-Shell, and Reducer-and-Shell Models" Modelling and Simulation in Engineering, Volume 2017, Article ID 9590214, 9 pages https://doi.org/10.1155/2017/9590214.
10. Shahab Bazri, Irfan Anjum Badruddin, Mohammad Sajad Naghavi, Ong Kok Seng, Somchai Wongwises, An analytical and comparative study of the charging and discharging processes in a latent heat thermal storage tank for solar water heater system, Solar Energy 185 (2019) 424–438.
11. F. M. Hussien, A. S. Hassoon, and J. J. Faraj, "Performance Analysis of a Triple Pipe Heat Exchanger with Phase Change Materials for Thermal Storage," International Journal of Heat and Technology, vol. 41, no. 3, pp. 619–628, Jun. 2023, doi: 10.18280/ijht.410314. Available: https://doi.org/10.18280/ijht.410314
12. Kadhim Hussein Suffer, Jalal M. Jalil, Hiba A. Hasan (2020). Numerical Investigation of PCM Thermal Storage in Water Solar Collector, Journal of Advanced Research in Fluid Mechanics and Thermal Sciences 66, Issue 1, 164-178.
13. Abdul Jabbar N. Khalifa, Kadhim H. Suffer, Mahmoud Sh. Mahmoud, A storage domestic solar hot water system with a back layer of phase change material, Experimental Thermal and Fluid Science 44 (2013) 174–181.
14. Ammar M. Abdulateef, Sohif Mat, Kamaruzzaman Sopian, Jasim Abdulateef, Ali A. Gitan" Experimental and computational study of melting phase-change material in a triplex tube heat exchanger with longitudinal/triangular fins" Solar Energy, Volume 155, October 2017, Pages 142-153.
15. Seddegh, Saeid, S. Saeed Mostafavi Tehrani, Xiaolin Wang, Feng Cao, and Robert A. Taylor. "Comparison of heat transfer between cylindrical and conical vertical shell-andtube latent heat thermal energy storage systems." Applied Thermal Engineering 130 (2018): 1349-1362.
16. Han, Guang-Shun, Hong-Sheng Ding, Yun Huang, Li-Ge Tong, and Yu-Long Ding. "A comparative study on the performances of different shell-and-tube type latent heat thermal energy storage units including the effects of natural convection." International Communications in Heat and Mass Transfer 88 (2017): 228-235.
17. Hiba A Hasan and Ihsan Y Hussain, "Theoretical formulation and numerical simulation of thermal performance enhancements for cascade thermal energy storage systems", IOP Conference Series: Materials Science and Engineering, vol. 433, no. 1, p. 012043. IOP Publishing, 2018.
18. A.Saraswat, A.Verma, S.Khandekar and M.K. Das, "Latent heat thermal energy storage in a heated semi-cylinder cavity: experimental results and numerical validation", Proceedings

of the 23rd National Heat and Mass Transfer Conf. (Thiruvananthapuram: India) Paper No. IHMTC- 862, Dec.2015.

19. H. A. Hasan, MK Abbas and JS Sherza, "Numerical Simulation for Using Winglet to Enhance the Airplane Wing Drag", Journal Of AL-Turath University College,Vol. 2, pp.113-123, Dec.2020.
20. B. Buonomo, O. Manca, D. Ercole and S. Nardini, "Numerical simulation of thermal energy storage phase change materials in aluminum foam" CLIMA - proceedings of the 12th REHVA World Congress (University of Naples II, Via Rome No. 29, 81031, Aversa (CE), Italy) vol 4, July.2016.
21. Nithyanandam K., Pitchumani R., "Computational Studies on Metal Foam and Heat Pipe Enhanced Latent Thermal Energy Storage", J. Heat Transfer, Vol. 136, 051503-1, 2014.
22. Soibam Jerol, "Numerical Investigation of a Phase Change Materials (PCM) heat exchanger", M.SC. Thesis, Norwegian University of Science and Technology, 2017.
23. H. A. Hasan and A. S. Hassoon, "Thermal performance investigation of finned latent heat storage of shell-and-tube, shell-and-nozzle, and shell-and-reducer models," *Heat Transfer*, vol. 52, no. 7, pp. 4755–4773, Jun. 2023, doi: 10.1002/htj.22906. Available: https://doi.org/10.1002/htj.22906
24. Korawan Agus Dwi, Sudjito Soeparman, Widya Wijayanti, and Denny Widhiyanuriyawan, "3D Numerical and Experimental Study on Paraffin Wax Melting in Thermal Storage for the Nozzle-and-Shell, Tube-and-Shell, and Reducer-and-Shell Models", Modelling and Simulation in Engineering Volume, Article ID 9590214, 9 pages, 2017.
25. Hesaraki A., "CFD Modeling of Heat Charging Process in a Direct-Contact Container for Mobilized Thermal Energy Storage", Thesis, Malardalen University, Sweden, 2011.
26. "Describing the uncertainties in experimental results," Describing the uncertainties in experimental results - ScienceDirect, Mar. 03, 2003 .
27. Z. Khan and Z. A. Khan, "An experimental investigation of discharge/solidification cycle of paraffin in novel shell and tube with longitudinal fins based latent heat storage system," Energy Conversion and Management, vol. 154, pp. 157–167, Dec. 2017.